Interplay of magnetism and superconductivity in the compressed Fe-ladder compound BaFe_{2}Se_{3}

Jianjun Ying, Hechang Lei, Cedomir Petrovic, Yuming Xiao, and Viktor V. Struzhkin

Phys. Rev. B **95**, 241109 — Published 20 June 2017

DOI: 10.1103/PhysRevB.95.241109

The interplay of magnetism and superconductivity in compressed Fe-ladder compound $BaFe_2Se_3$

Jianjun Ying,[1,2] Hechang Lei,[3,*] Cedomir Petrovic,[3] Yuming Xiao,[2] and Viktor V. Struzhkin[1,†]

[1]*Geophysical Laboratory, Carnegie Institution of Washington, Washington, DC 20015, USA.*
[2]*HPCAT, Geophysical Laboratory, Carnegie Institution of Washington, Argonne, Illinois 60439, USA*
[3]*Condensed Matter Physics and Materials Science Department, Brookhaven National Laboratory, Upton, New York 11973, USA*

(Dated: March 28, 2017)

High pressure resistance, susceptibility and Fe K_β x-ray emission spectroscopy measurements were performed on a Fe-ladder compound $BaFe_2Se_3$. The pressure-induced superconductivity was observed which is similar to the previously reported superconductivity in the $BaFe_2S_3$ samples. The slope of local magnetic moment versus pressure shows anomaly across the insulator-metal transition pressure in the $BaFe_2Se_3$ samples. The local magnetic moment is continuously decreasing with increasing pressure, and the superconductivity appears only when the local magnetic moment value is comparable to the one in the iron-pnictide superconductors. Our results indicate that the compressed $BaFe_2Ch_3$ (Ch=S, Se) is a new family of iron-based superconductors. Despite the crystal structures completely different from the known iron-based superconducting materials, the magnetism in this Fe-ladder material plays a critical role in superconductivity. This behavior is similar to the other members of iron-based superconducting materials.

PACS numbers:

Iron-based superconductors provide a fertile playground for sorting out the effects of the magnetic degree of freedom on the superconductivity[1, 2]. The magnetic fluctuations instead of electron-phonon coupling were suggested as a pairing glue in the iron-based superconductors[3, 4]. Both a local moment scenario and itinerant models have been invoked to establish the nature of magnetism in these materials[5]. The iron-based superconductors have been interpreted as a family of materials in a proximity to a Mott transition, similar to the cuprate materials [6–8], which favors the local moment approach. Thus, directly probing the local magnetic moment is a crucial component in solving the mechanism of the high T_C superconductivity in iron-based superconductors. The neutron scattering is usually used to detect the local magnetic moments. However, it requires a large quantity of sample, thus limiting its application, especially in the high pressure experiments. A bulk-sensitive method of x-ray emission spectroscopy (XES), which can detect the local magnetic moment of Fe in small samples, has been proven to be a useful method to quantitatively obtain the information on the local magnetic moment of Fe and other transition metal materials.[9–12]. Although many families of iron-based superconductors have been discovered until now, the majority of the iron-based superconductors have a two-dimensional Fe-square lattice tetrahedrally coordinated by pnictogens or chalcogens. Recently, pressure induced superconductivity was observed in an one-dimensional Fe-ladder compound $BaFe_2S_3$[13, 14], which provided a quasi-one dimensional structural prototype for the studies of iron-based superconductors. However, whether such superconductivity is universal in one-dimensional Fe-ladder compounds is still unknown. Since high pressure is needed to induce the superconductivity, a limited number of the experimental methods can be used in studies of this material. It remains unknown, whether the mechanism of superconductivity in $BaFe_2S_3$ is similar to the one in other two-dimensional iron-based superconductors. In this letter we report our results on a similar compound which help to solve these problems.

The two-leg ladder $BaFe_2Se_3$ compound is a semiconductor with the long-range antiferromagnetic (AFM) order around T_N = 250 K[15–17]. It adopts the $CsAg_2I_3$-type structure (Pnma space group), which can be considered as the distorted $BaFe_2S_3$ (Cmcm space group) structure. Each unit cell has two iron ladders along b-direction which are built by edge-sharing $FeSe_4$ tetrahedra. The $BaFe_2Se_3$ hosts an exotic block magnetic order with magnetic moments (2.8μB/Fe) aligned perpendicular to the leg direction[19–21] (which is analogous to the block AFM order in $K_xFe_{1.6}Se_2$[22]) , in contrast to the other 123-ladder compounds and the iron-pnictide superconductors, which exhibit stripe magnetic order[19, 23, 24]. It is proposed that $BaFe_2Se_3$ forms an orbital-selective Mott phase and is a potential magnetic multiferroic with a large ferroelectric polarization, as predicted by theory[25, 26]. By applying pressure, a structural transition is induced around 6 GPa, transforming the material to a structure similar to $BaFe_2S_3$[18] at high pressure. However, whether superconductivity can be induced and how the magnetic moments will evolve under pressure, is still unknown in this material.

By using the high pressure transport, susceptibility and XES measurements, we can map out the phase diagram and check whether the compressed $BaFe_2Se_3$ is a superconductor. We can also obtain the information on the local magnetic moment on Fe from the XES mea-

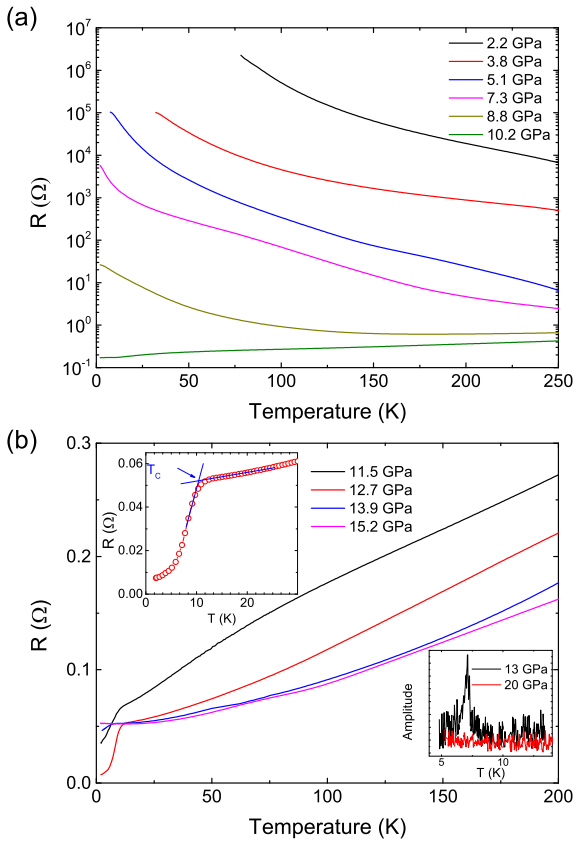

FIG. 1: (color online). The temperature dependence of the resistance of $BaFe_2Se_3$ at various pressures. (a) The resistance is gradually suppressed during compression. The metallic behavior emerges above 7 GPa. (b) An anomaly around 11 K appears in the metallic state which is possibly due to the superconducting transition. The transition becomes quite sharp around 12.7 GPa. The superconducting transition can be completely suppressed by applying high pressures above 15 GPa. The upper inset shows in more detail the resistance around the T_C. The lower inset shows the magnetic inductive measurements of the sample with superconductivity (black line) and without superconductivity (red line).

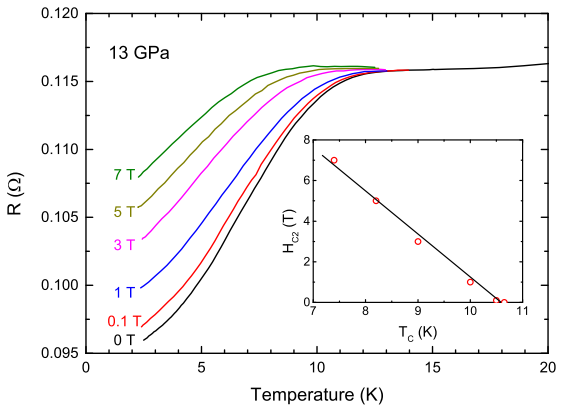

FIG. 2: (color online). The temperature dependence of the resistance of the $BaFe_2Se_3$ sample at various magnetic fields under the pressure of 13 GPa. The deduced upper critical field (H_{C2}) is shown in the inset.

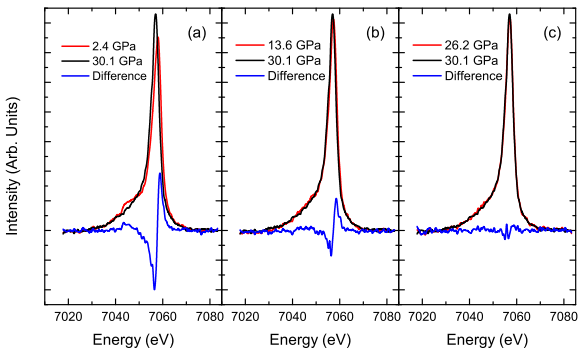

FIG. 3: (color online). The normalized room-temperature XES at Fe K_β for $BaFe_2Se_3$ at the pressure of (a) 2.4 GPa, (b) 13.6 GPa and (c) 26.2 GPa as compared with the spectrum at 30.1 GPa(black line). The difference of the spectra between 26.2 GPa and 30.1 GPa is rather small, thus we can assume the system is completely tuned to non-magnetic state above 30 GPa.

surements under pressure, which is a crucial contribution to the understanding of the novel properties of these one dimensional ladder compounds under pressure. These results will also help us to understand how the magnetism is coupled to the superconductivity in iron-based superconductors.

High quality single crystals of $BaFe_2Se_3$ were grown by self-flux method[15]. Pressure was applied at room temperature using the miniature diamond anvil cell for resistance measurement[27]. Leads are insulated from Re gasket with *c*-BN\epoxy mixture[28]. Diamond anvils with 300 μm culet with sample chambers of diameter 120 μm were used. KCl was used as the pressure transmitting medium. Pressure was calibrated by using the ruby fluoresce shift at room temperature. The current is applied in the *bc* plane and the magnetic field is applied along the *a*-axis direction. Resistance was measured using the Quantum Design PPMS-9. A single crystal cut with the dimensions of $65\times65\times10$ μm^3 was used for the magnetic susceptibility measurement. Two single loop coils made with 2μm thick gold foil were attached on the culets of the two diamonds respectively. The single loop coils were insulated from Re gasket with *c*-BN\epoxy mixture. One single loop coil was used as the excitation coil with frequency around 10∼20MHz. The other one was used as signal coil. The low frequency modulating coil was wrapped around the cell[29]. The diamond anvils with

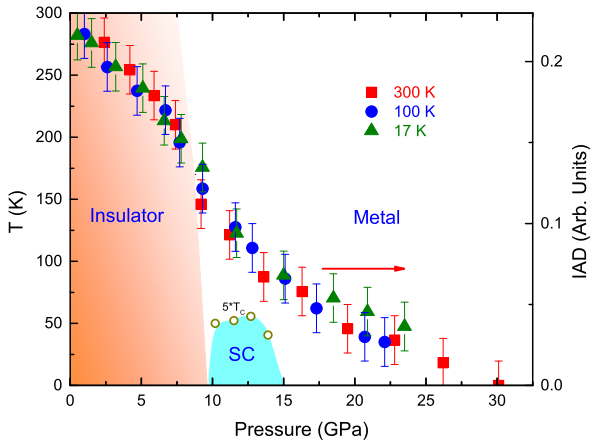

FIG. 4: (color online). The phase diagram of $BaFe_2Se_3$ under pressure. The deduced IAD which is proportional to the Fe local moment is shown as the red squares (300 K), blue circles(100 K) and green triangles (17 K) . The slope of magnetic moment of Fe versus pressure shows anomaly around the pressure at which insulator-metal transition takes place. Further increasing the pressure, the magnetic moment keep decreasing and superconducting transition appears at low temperature.

300 μm culets and Be gasket were used for the x-ray emission spectroscopy (XES) measurements. The XES measurements were performed at the 16-IDD beamline of the High-Pressure Collaborative Access Team (HPCAT) at the Advanced Photon Source at the Argonne National Laboratory.

The temperature dependence of the resistance under high pressure for $BaFe_2Se_3$ is shown in Figure 1. The resistance shows insulating behavior at low pressures. The resistance gradually decreases under compression and an insulator-metal transition starts to appear above 7.3 GPa. At the pressure around 8.8 GPa, insulator-metal transition temperature shifts to 150 K. Above 10.2 GPa, the resistance shows a metallic behavior in the whole temperature range. Meanwhile, the resistance shows a sudden decrease around 11 K, which is possibly due to the superconducting transition. This transition becomes very sharp at pressures around 12.7 GPa, and disappears above 15 GPa. A non-zero resistance is possibly due to the non-hydrostatic pressure in the diamond anvil cell with the solid pressure medium: such behavior is similar to the $BaFe_2S_3$ case[13]. We detected also the susceptibility signal by using the inductive modulation method[29] as shown in the lower inset of Fig.1(b). The peak emerges under 13 GPa which is due to the superconducting transition. Susceptibility signal shows no sign of transition at 20 GPa when the superconductivity is completely suppressed.

In order to confirm the superconducting transition, we have applied the magnetic field to suppress the transition temperature. Temperature dependence of the resistance of the $BaFe_2Se_3$ sample at various magnetic fields under the pressure of 13 GPa is shown in Figure 2. The increasing magnetic field gradually suppresses the transition temperature, which is typical for the superconducting transition. From these measurements, we obtain the upper critical field (H_{C2}), which is shown in the inset of Fig. 2. The T_c was determined from the onset of the resistance drop similar with the inset of Fig.1 (b). Within the weak-coupling BCS theory, the upper critical field at T = 0 K can be determined by the Werthamer-Helfand-Hohenberg (WHH) equation [31] $H_{c2}(0) = 0.693[-(dH_{c2}/dT)]_{T_c}T_c$. We can deduce that $H_{c2}(0)\sim$15.5 T. The combined transport and susceptibility measurements confirm the superconductivity in the compressed $BaFe_2Se_3$. Our result contrasts with a recent high pressure work on $Ba_{1-x}Cs_xFe_2Se_3$[35], where no superconductivity or metallization in $BaFe_2Se_3$ is observed. Such discrepancy is possibly due to the difference in the original crystals. The small difference in Ba or Fe content may dramatically alter the physical properties. Further high pressure works are needed to solve this discreapancy.

As we know, $BaFe_2Se_3$ exhibits AFM order below 250 K with the large local magnetic moments on iron sites. It is crucial to study the evolution of magnetic moments under pressure, especially in the superconducting state. However, the common magnetic measurements methods, such as neutron scattering, need a large sample volume which is difficult to accommodate under conditions of high pressure experiments. In order to obtain the information about the local magnetic moments under pressure, we have performed the Fe K_β XES measurements, which can probe directly the local magnetic moment on the Fe site. In order to quantitatively derive the total local moment from the K_β line profile, we have used the integrated absolute difference (IAD) analysis, which has been successfully performed on the other layered iron-based superconductors[10–12]. In order to obtain IAD values, a reference sample with the same local coordination around Fe without a local magnetic moment is needed. However, such low-spin samples with the structure similar to $BaFe_2Se_3$ are not available. In order to obtain the IAD, we have used the spectrum which is taken at 30.1 GPa as a reference, since high pressure is known to suppress the local magnetic moments in Fe-based materials[10, 32]. The Figure 3 shows the typical normalized room-temperature XES of Fe K_β spectral lines for $BaFe_2Se_3$ under pressure. We notice that the difference of the spectra between 26.2 GPa and 30.1 GPa is rather small, supporting our assumption that the system has been completely tuned to a non-magnetic state above 30 GPa.

We can map out the phase diagram as shown in figure 4. The deduced IAD value (proportional to the local magnetic moment) gradually decreases with increasing

pressure. The initial IAD value is equal to the value measured in $A_2Fe_4Se_5$ (A=K, Rb, Cs) at low pressures[12]. Previous results indicate that the magnetic moment of $BaFe_2Se_3$ is about 2.8 μB, which is smaller than the magnetic moment of $A_2Fe_4Se_5$ (3.3 μB). The photoemission spectroscopy also reveals the coexistence of the localized and itinerant electrons in $BaFe_2Ch_3$[33]. Such small discrepancy is due to the local Fe environment in $BaFe_2Se_3$ being different to the one in the layered iron-based superconductors, thus the overall scaling factor is slightly different. The slope of IAD value shows anomaly around 7.5 GPa, near the insulator-metal transition in the sample. This pressure is also quite close to the pressure at which the structural transition occurs[18]. By increasing the pressure, the bandgap is gradually decreased, and the local moment gradually becomes itinerant. The superconductivity emerges for the IAD value between 0.06 and 0.1 ($\sim$0.7 μB to 1.3 μB). The deduced magnetic moment is similar to the one in the iron-pnictide superconductors[12]. The IAD value becomes small after the superconducting transition is completely suppressed. These results indicate that the magnetism plays an important role in the superconductivity and the mechanism of the superconductivity for the $BaFe_2Se_3$ might be similar to the other iron-based superconductors. We also performed high pressure XES measurements at low temperatures as shown in Figure 4. The IAD values measured at the temperatures of 17 K and 100 K exhibit the same pressure dependence as the room temperature data, which indicates that the local moment almost does not change with the temperature. The critical pressure at which the IAD value drops is shifting to a slightly higher pressure when the temperature is decreased. It is consistent with the insulator-metal transition shown in Figure 1.

The observed insulator-metal transition takes place when the local magnetic moment is decreasing. The critical pressure at room temperature is also quite close to the structural transition reported previously[18]. Our results support the intimate relation between the magnetism, the crystalline lattice, and the electronic structure in this material. The magnetoelastic coupling was suggested as the origin of the structural distortion at ambient pressure[17]. The decrease of the magnetic moment will greatly decrease the magnetoelastic coupling, thus, within this model, the structure will become less distorted, and similar to the structure of the $BaFe_2S_3$ compound at high pressures. The discovery of the superconductivity in compressed $BaFe_2Se_3$ confirms that the $BaFe_2Ch_3$ (Ch=S, Se) is a new family of iron-based superconductors, which are similar to the Cu-oxide ladders that are also superconducting[34]. The exotic magnetic and superconducting properties make these 123-ladder compounds an ideal playground to explore the correlations between the magnetism and superconductivity. By doping K or Cs in $BaFe_2Se_3$ material, the crystal structure can also be tuned to $BaFe_2S_3$-type structure[19, 35]. Meanwhile, in such doped materials, the block magnetic structures change to the strip magnetic structures, which may be similar to our high pressure case. Although we can not deduce the magnetic structure from our XES results, the block AFM structure may also change to the stripe AFM structure after structural transition. High pressure neutron scattering measurements are needed to confirm this assumption. The maximum T_C in $BaFe_2Se_3$ is lower than the T_C in $BaFe_2S_3$, which is different from the other layered iron-chalcogenide superconductors in which the T_C in FeSe-based materials is much higher than the T_C in FeS superconductors[36–38]. It is a possible that the T_C in the $BaFe_2Se_3$ material is not optimized, and small local modifications of the structure of $FeSe_4$ tetrahedra may help to increase the T_C.

In conclusion, we have observed the insulator-metal transition in the compressed Fe-ladder compound $BaFe_2Se_3$, which is accompanied by the change in the Fe local magnetic moment dependence versus pressure. The superconductivity emerges above 10 GPa, which is similar to the behavior of the $BaFe_2S_3$ material. The superconductivity has strong correlation with the magnitude of the local magnetic moment of iron. Our results directly show that the relatively small magnitude of the local magnetic moments is crucial to the occurrence of the superconductivity in this one dimensional Fe-ladder compound. This behavior is similar to the other layered iron-based superconductors, which supports the similarity in the mechanisms of the superconductivity despite the different structural motives in the iron-based superconductors.

High pressure experiments at HPCAT were supported by DOE/BES under contract No. DE-FG02-99ER45775. Portions of this work were performed at HPCAT (Sector 16), Advanced Photon Source (APS), Argonne National Laboratory. HPCAT operation is supported by DOE-NNSA under Award No. DE-NA0001974, with partial instrumentation funding by NSF. The Advanced Photon Source is a U.S. Department of Energy (DOE) Office of Science User Facility operated for the DOE Office of Science by Argonne National Laboratory under Contract No. DE-AC02-06CH11357.

* Present address Department of Physics, Renmin University, Beijing 100872, Peoples Republic of China
† Electronic address: vstruzhkin@carnegiescience.edu

[1] M. D. Lumsden and A. D. Christianson, J. Phys. Condens. Matter **22**, 203203 (2010).
[2] P. Dai, J. Hu, and E. Dagotto, Nat. Phys. **8**, 709 (2012).
[3] A. V. Chubukov, Annu. Rev. Condens. Matter Phys. **3**, 57C92 (2012).
[4] P. J. Hirschfeld, M. M. Korshunov, I. I. Mazin, Rep. Prog. Phys. **74**, 124508 (2011)

[5] J. Paglione, and R. L. Greene, Nat. Phys. **6**, 645 (2010).
[6] Q. Si and E. Abrahams, Phys. Rev. Lett. **101**, 076401 (2008).
[7] R. Yu and Q. Si, Phys. Rev. Lett. **110**, 146402 (2013).
[8] L. de Medici, G. Giovannetti, and M. Capone, Phys. Rev. Lett. **112**, 177001 (2014).
[9] J.-P. Rueff, C. C. Kao, V. V. Struzhkin, J. Badro, J. Shu, R. J. Hemley, and H. K. Mao, Phys. Rev. Lett. **82**, 3284 (1999).
[10] J. P. Rueff, M. Krisch, Y. Q. Cai, A. Kaprolat, M. Hanfland, M. Lorenzen, C. Masciovecchio, R. Verbeni, and F. Sette, Phys. Rev. B **60**, 14510 (1999).
[11] G. Vankó, T. Neisius, G.Molnar, F. Renz, S. Karpati, A. Shukla, and F. M. F. de Groot, J. Phys. Chem. B **110**, 11647 (2006).
[12] H. Gretarsson, A. Lupascu, J. Kim, D. Casa, T. Gog, W. Wu, S. R. Julian, Z. J. Xu, J. S. Wen, G. D. Gu, R. H. Yuan, Z. G. Chen, N.-L.Wang, S. Khim, K. H. Kim, M. Ishikado, I. Jarrige, S. Shamoto, J.-H. Chu, I. R. Fisher, and Y.-J. Kim, Phys. Rev. B **84**, 100509(R) (2011).
[13] H. Takahashi, A. Sugimoto, Y. Nambu, T. Yamauchi, Y. Hirata, T. Kawakami, M. Avdeev, K. Matsubayashi, F. Du, C. Kawashima, H. Soeda, S. Nakano, Y. Uwatoko, Y. Ueda, T. J. Sato, and K. Ohgushi, Nature Materials, **14**, 1008 (2015).
[14] T. Yamauchi, Y. Hirata, Y. Ueda, and K. Ohgushi, Phys. Rev. Lett. **115**, 246402 (2015).
[15] H. Lei, H. Ryu, A. I. Frenkel, and C. Petrovic, Phys. Rev. B **84**, 214511 (2011).
[16] A. Krzton-Maziopa, E. Pomjakushina, V. Pomjakushin, D. Sheptyakov, D. Chernyshov, V. Svitlyk, and K. Conder, J. Phys. Condens. Matter **23**, 402201 (2011).
[17] J. M. Caron, J. R. Neilson, D. C. Miller, A. Llobet, and T. M. McQueen, Phys. Rev. B **84**, 180409(R) (2011).
[18] V. Svitlyk, D. Chernyshov, E. Pomjakushina, A. KrztonMaziopa, K. Conder, V. Pomjakushin, R. Pottgen, V. Dmitriev, Journal of Physics-Condensed Matter **25**, 315403 (2013).
[19] J.M. Caron,J. R. Neilson, D. C. Miller, K. Arpino, A. Llobet, and T. M. McQueen, Phys. Rev. B **85**, 180405(R) (2012).
[20] Y. Nambu, K. Ohgushi, S. Suzuki, F. Du, M. Avdeev, Y. Uwatoko, K. Munakata, H. Fukazawa, S. Chi, Y. Ueda, and T. J. Sato, Phys. Rev. B **85**, 064413 (2012).
[21] M. Mourigal, S. Wu, M. Stone, J. Neilson, J. Caron, T. McQueen, and C. Broholm, Phys. Rev. Lett. **115**, 047401 (2015).
[22] F. Ye, S. Chi, W. Bao, X. F. Wang, J. J. Ying, X. H. Chen, H. D.Wang, C. H. Dong, and M. Fang, Phys. Rev. Lett. **107**, 137003 (2011).
[23] F. Du, K. Ohgushi, Y. Nambu, T. Kawakami, M. Avdeev, Y. Hirata, Y. Watanabe, T. J. Sato, and Y. Ueda, Phys. Rev. B **85**, 214436 (2012).
[24] Songxue Chi, Yoshiya Uwatoko, Huibo Cao, Yasuyuki Hirata, Kazuki Hashizume, Takuya Aoyama, Kenya Ohgushi, arXiv:1606.09223
[25] J. Rincón, A. Moreo, G. Alvarez, and E. Dagotto, Phys. Rev. Lett. **112**, 106405 (2014).
[26] S. Dong, J.-M. Liu, and E. Dagotto, Phys. Rev. Lett. **113**, 187204 (2014).
[27] A. G. Gavriliuk, A. A. Mironovich, and V. V. Struzhkin, Rev. Sci. Instrum. **80**, 043906 (2009).
[28] M. I. Eremets, V. V. Struzhkin, H. K. Mao, R. J. Hemley, Science **293**, 272 (2001).
[29] Yu. A. Timofeev, V. V. Struzhkin, R. J. Hemley, H. K. Mao, and E. Gregoryanz, Rev. Sci. Instrum. **73**, 371 (2002).
[30] T. Hawai, C. Kawashima, K. Ohgushi, K. Matsubayashi, Y. Nambu, Y. Uwatoko, T. J. Sato, and H. Takahashi, J. Phys. Soc. Jpn. **86**, 024701 (2017).
[31] N. R. Werthamer, E. Helfand, and P. C. Hohenberg, Phys. Rev. **147**, 295-302 (1966).
[32] J. R. Jeffries, N. P. Butch, M. J. Lipp, J. A. Bradley, K. Kirshenbaum, S. R. Saha, J. Paglione, C. Kenney-Benson, Y. Xiao, P. Chow, and W. J. Evans, Phys. Rev. B **90**, 144506 (2014).
[33] D. Ootsuki, N. L. Saini, F. Du, Y. Hirata, K. Ohgushi, Y. Ueda, and T. Mizokawa, Phys. Rev. B **91**, 014505 (2015).
[34] E. Dagotto, Rep. Prog. Phys. **62**, 1525 (1999).
[35] Takafumi Hawai, Yusuke Nambu, Kenya Ohgushi, Fei Du, Yasuyuki Hirata, Maxim Avdeev, Yoshiya Uwatoko, Yurina Sekine, Hiroshi Fukazawa, Jie Ma, Songxue Chi, Yutaka Ueda, Hideki Yoshizawa, and Taku J. Sato, Phys. Rev. B **91**, 184416 (2015).
[36] F.C. Hsu, J. Y. Luo, K.W. Yeh, T. K. Chen, T.W. Huang, Phillip M. Wu, Y.C. Lee, Y. L. Huang, Y. Y. Chu, D. C. Yan, and M. K. Wu, Proc. Natl. Acad. Sci. USA **105**, 14262, (2008).
[37] S. Medvedev, T. M. McQueen, I. A. Troyan, T. Palasyuk, M. I. Eremets, R. J. Cava, S. Naghavi, F. Casper, V. Ksenofontov, G.Wortmann, and C. Felser, Nature Mater. **8**, 630 (2009).
[38] Xiaofang Lai, Hui Zhang, Yingqi Wang, Xin Wang, Xian Zhang, Jianhua Lin, and Fuqiang Huang, J. Am. Chem. Soc. **137**, 10148-10151 (2015).